Published in final edited form as:
Neuroscience. 2011 September 8; 190: 398–408. doi:10.1016/j.neuroscience.2011.06.010.

Dcdc2 knockout mice display exacerbated developmental disruptions following knockdown of *Dcx*

Yu Wang[1], **Xiuyin Yin**[1], **Glenn Rosen**[2], **Lisa Gabel**[3], **Sarah M. Guadiana**[4], **Matthew R Sarkisian**[4], **Albert M. Galaburda**[2], and **Joseph J. LoTurco**[1,*]

[1]Department of Physiology and Neurobiology, University of Connecticut, Storrs CT 06269

[2]The Dyslexia Research Laboratory, Division of Behavioral Neurology, Department of Neurology, Beth Israel Deaconess Medical Center, 330 Brookline Avenue, Boston, MA 02215, USA

[3]Department of Psychology, Lafayette College, Easton PA

[4]Department of Neuroscience, McKnight Brain Institute, University of Florida, Gainesville, FL 32610-0244

Abstract

The dyslexia-associated gene *DCDC2* is a member of the *DCX* family of genes known to play roles in neurogenesis, neuronal migration and differentiation. Here we report the first phenotypic analysis of a *Dcdc2* knockout mouse. Comparisons between *Dcdc2* knockout mice and wild type littermates revealed no significant differences in neuronal migration, neocortical lamination, neuronal cilliogenesis or dendritic differentiation. Considering previous studies showing genetic interactions and potential functional redundancy among members of the *DCX* family, we tested whether decreasing *Dcx* expression by RNAi would differentially impair neurodevelopment in *Dcdc2* knockouts and wild type mice. Consistent with this hypothesis, we found that deficits in neuronal migration, and dendritic growth caused by RNAi of *Dcx* were more severe in *Dcdc2* knockouts than in wild type mice with the same transfection. These results indicate that *Dcdc2* is not required for neurogenesis, neuronal migration or differentiation in mice, but may have partial functional redundancy with *Dcx*.

Introduction

Genetic variation in *DCDC2* in humans has been associated with developmental learning disabilities including reading disability (Meng H et al., 2005; Schumacher J et al., 2006), attention deficit hyperactivity disorder (ADHD) (Couto JM et al., 2009), and difficulties in mathematics (Marino C et al.). A genetic variant of *DCDC2* associated with dyslexia in some studies is present within an enhancer region that regulates *DCDC2* expression (Meng H et al., 2010), further suggesting that altered expression of *Dcdc2* may be related to developmental learning disability. The specific cellular function or functions of *Dcdc2* protein in development and physiology are currently not well characterized, although its

*Corresponding Author: Joseph LoTurco, Department of Physiology and Neurobiology, University of Connecticut, Storrs, 06269, Joseph.LoTurco@UConn.edu, Phone: 860-487-5421.

structural relatedness to doublecortin (*Dcx*) family members, and results from *in vivo* RNAi studies in rats, suggest that *Dcdc2* may play a role in neuronal migration.

Dcdc2 is ubiquitously expressed in developing rodent and mature human neocortex (Burbridge TJ et al., 2008; Meng H *et al*., 2005), and could potentially have roles in several aspects of neural development and/or function. RNAi of *Dcdc2* in subpopulations of migrating neocortical neurons in developing rat neocortex causes deficits in neuronal migration indicating that at least one function of *Dcdc2*, similar to other members of the *Dcx* family, may be in neuronal migration (Burbridge TJ *et al.*, 2008; Meng H *et al.*, 2005). Similarly, *Dcdc2* protein interacts with many of the same cytoskeleton related proteins that other members of the *Dcx* family interact with, including tubulin, suggesting that *Dcdc2* could have a role in mechanisms of cell migration or differentiation that require cytoskeletal dynamics (Reiner O et al., 2006). Loss-of-function mutations in mice of members of the *Dcx* family--*Dcx*, *Dclk1* and *Dclk2*--cause alterations in neuronal migration, neurogenesis and/or dendritic differentiation (Corbo JC et al., 2002; Kerjan G et al., 2009; Pramparo T et al., 2010). Results from analysis of compound mutants of members of the *Dcx* family indicate that members of the family genetically interact and may participate in coordinated function during neurodevelopment (Deuel TA et al., 2006; Koizumi H et al., 2006).

In this study we produced and analyzed the first knockout mouse of *Dcdc2* in the mouse (*Dcdc2a*). *Dcdc2* knockout mice are healthy and breed normally. Neurogenesis, neuronal migration, and lamination of neocortex are not significantly different between *Dcdc2* knockouts and wild type animals. We also used *in utero* RNAi targeted against *Dcx* in developing neocortex in homozygous wildtype and homozygous *Dcdc2* mutant animals to investigate a potential shared function between *Dcx* and *Dcdc2*. *Dcx* RNAi created more developmental disruption in *Dcdc2* knockouts than in wt mice. The enhanced disruptions included the appearance of subcortical band heterotopia and disruptions in dendritic growth. These results show that genetic loss of *Dcdc2* does not alone create abnormalities in neuronal migration or differentiation in neocortex, but that *Dcdc2* may have partial functional redundancy with *Dcx* in regulating neuronal migration and dendritic growth, which is revealed only after both are rendered dysfunctional. The *Dcdc2* mutant mouse presents the opportunity for future studies into the role or roles of *Dcdc2* in behavior and physiology that are independent of disruptions in neuronal migration.

Results

Targeted genetic deletion of *Dcdc2*

In order to generate *Dcdc2* mutant mice we sequentially generated mouse lines bearing engineered *Dcdc2* alleles; a conditional deletion or “floxed” allele in which exon 2 was flanked by loxp sites, $Dcdc2^{flox2}$, and a constitutively deleted allele in which exon2 was deleted, $Dcdc2^{del2}$((figure 1 A&B). Deletion of exon 2, an exon present in all annotated splice variants of *Dcdc2*, is predicted to result in a frame shift and premature stop codon when exon 1 and exon 3 are spliced together. To verify this aberrant splice variant and stop codon in the mutants we used RT-PCR with primers to exon 1 and exon 3, sub-cloned, and then sequenced the resulting fragments. As shown in figure 1C, consistent with loss of the 52 base pair exon 2, the amplified product from homozygous mutant animals ($Dcdc2^{del2/del2}$) was approximately 50 bases smaller than that amplified from $Dcdc2^{wt/wt}$ animals (figure 1C). Furthermore, the sequence of the amplified fragment from homozygous mutants indicated that the exon 1-to-exon 3 spliced sequences contained the expected premature stop codon (figure 1D). Introduction of premature stop codons by mutation often result in transcripts that are degraded by nonsense-mediated mRNA decay. We tested for such decay by quantitative rt PCR ((qPCR) to determine whether *Dcdc2* mRNA levels were lower in mice with alleles missing exon 2. In cDNA prepared from RNA isolated from the

brains of homozygous mutants we found evidence of approximately 10 fold decrease in *Dcdc2* mRNA than in *Dcdc2*$^{wt/wt}$ animals. Similarly, in heterozygous animals, with one mutant and one wt allele, we found intermediate levels of *Dcdc2* mRNA. These results are consistent with potent nonsense mediated decay and loss of *Dcdc2* transcripts in *Dcdc2*$^{del2/del2}$ mutant mice (figure 1E; N=21 $p<0.001$). We also attempted to confirm decreased expression at the protein level, however five commercially purchased and tested antibodies failed to identify bands of the appropriate MW for *Dcdc2* even in wild type brains. Nevertheless, the aberrant splice variant, premature stop codon, and potent nonsense-mediated decay in the mutant provide substantial evidence that the *Dcdc2*^{del2} is a loss of function mutant allele for *Dcdc2*.

In crosses between mice heterozygous for the *del2* and *wt* alleles of *Dcdc2*, as well as in crosses between animals homozygous and heterozygous for the *del2* alleles, we observed the expected mendelian ratios of 1:2:1 and 1:1 respectively, indicating no evidence of embryonic lethality associated with *Dcdc2*^{del2}. Animals homozygous for the *del2* deletion are healthy and are fertile. As an initial screening for behavioral changes in *Dcdc2* knockout mice we tested *Dcdc2*$^{del2/del2}$, *Dcdc2*$^{wt/del2}$, and *Dcdc2*$^{wt/wt}$ mice on open field behavior and on one configuration of the Hebb-Williams maze (maze 1). As shown in figure 1 F&G, there were no significant behavioral differences in either behavioral test. Measures of spontaneous locomotion and exploratory behavior in the open field test showed no significant differences (Figure 1; $p >0.05$). Similarly, there was no significant difference in performance on Maze 1 of the Hebb-Williams maze, with no significant interaction between trial and genotype for the number of errors committed during testing ($p >005.$), and no significant main effect of genotype ($p> 0.05$) in learning the maze. There was, however, a significant main effect of trial across genotypes, confirming that animals learned the task ($p< 0.05$).

Dcdc2 mutants have structurally normal brains

Dcdc2 knockout mice showed no defects in brain morphology as assessed by comparison of serially sectioned brains from *Dcdc2*$^{wt/wt}$ and *Dcdc2*$^{del2/del2}$ mice (figure 2 A,B). Laminated neural structures, including neocortex, hippocampus and cerebellum, all showed typical morphologies. Similarly, the size and organization of major white matter tracts showed no evidence of disruption. There was also no evidence of focal developmental disruptions in neocortex, including neither periventricular heterotopia nor layer 1 ectopia. In addition, the numbers of total neuronal and non-neuronal cells in the cerebral neocortex, as assessed by non-biased stereology of Nissl-stained sections, showed no significant differences between wild type and knockout mice. Furthermore, immunohistochemistry of two neocortical-layer specific markers, Cux1 (layers II–IV) and Tbr1 (layer V and VI) revealed no significant differences in neocortical lamination patterns (figure 2 C&D).

As *Dcdc2* has been shown to bind to microtubules, and *Dcdc2* expressed in hippocampal neurons, localizes to neuronal cilia and alters cilia signaling (Massinen et al, in press), we performed an assessment of neuronal cillia in hippocampus and cerebral cortex in P54 Dcdc2^{wtwt} and Dcdc2$^{del2/del}$ mice. Neuronal cilia can be identified immunocytochemically due to their enriched expression of type III adenylyl cyclase and pericentrin, proteins localized to the axoneme and basal body, respectively (Bishop et al., 2007, Anastas et al., 2011). We therefore performed an immunocytochemical assessment of neuronal cilia in hippocampus and neocortex of 54 day old *Dcdc2*$^{del2/del2}$ and *Dcdc2*$^{wt/wt}$ mice. However, the structure, numbers, and lengths of neuronal cilia in neocortex and hippocampus did not differ between *Dcdc2*$^{del2/del2}$ and *Dcdc2*$^{wt/wt}$ mice (figure 3). Further studies are needed to determine whether signaling to or from these cilia is altered in *Dcdc2* mutants.

Dcdc2 mutants display normal neocortical neurogenesis and neuronal migration

Recent reanalysis of *Dcx* knockout mice, which were initially shown to have undisturbed neocortical lamination (Corbo JC *et al.*, 2002), revealed significant changes in both neurogenesis and neuronal migration in fetal development in *Dcx* mutants that were largely resolved and no longer apparent by later postnatal periods (Pramparo T *et al.*, 2010). We therefore investigated both neurogenesis and migration during the fetal period in *Dcdc2* knockouts. To assess neurogenesis, we compared the percentage of neocortical progenitors within the VZ that were in M-phase of the cell cycle (phoH3+ cells) at embryonic day 15 (E15). We found no significant differences between wild type and *Dcdc2* knockout mice (figure 4A). We also tested whether *Dcdc2* loss altered the fraction of neocortical progenitor cells that exit the cell cycle. For this analysis, BrdU injections were made at E15, and brains were harvested and processed for BrdU and Ki67 immunohistochemistry 24 hours later. The percentage of cells that had exited the cell cycle after 1 day, $BrdU^+$ and $Ki67^-$ cells, did not significantly differ between $Dcdc2^{wt/wt}$ and $Dcdc2^{del2/del2}$ mice (figure 4A). Together these results indicate that the number of mitotic neural progenitors or the rate at which neocortical neuronal progenitors become postmitotic is not altered by the *Dcdc2* deletion mutation.

In order to test whether there were any defects in neuronal migration in *Dcdc2* mutants, we performed three different experiments. First, we injected pregnant females at gestational day 15 with BrdU and examined the positions of BrdU positive neurons within neocortex on the day of birth. As shown in Figure 3C, in both wild-type and knockout mice, BrdU labeled cells reached the top of the cortical plate revealing no apparent migration delays or arrest. In an additional assay for migration, we used electroporation of VZ progenitors at the ventricular zone at E15 to label migrating neurons with GFP and then assessed the position of neurons on the day of birth. Similar to the BrdU assay, GFP labeled neurons were present in upper layers in both knockouts and wt mice (figure 4D). Lastly, to test whether cells lacking a functional copy of *Dcdc2* would migrate more slowly if migrating within the context of a population of cells with functional *Dcdc2* alleles we used animals homozygous for the $Dcdc2^{flox2}$ allele and transfected these $Dcdc2^{flox2/flox2}$ animals at E15 with plasmids expressing cre, pCAG-Cre, and a conditionally gated GFP, pCALNL-GFP. Cre-transfected cells in wild type and in $Dcdc2^{flox/flox}$ animals were marked by the expression of GFP and these cells migrated similarly from the VZ to superficial layers of neocortex (figure 4E) in both $Dcdc2^{flox2/flox2}$ and $Dcdc2^{wt/wt}$. Together, the results of these three neuronal migration assays indicate that genetic deletion of *Dcdc2* in mice does not result in impaired neuronal migration of pyramidal neurons in mouse neocortex.

Dcx RNAi impairs neuronal migration more in *Dcdc2* knockouts than in wildtype mice

Previous studies of compound *Dcx* and dclk1 mutations in mice indicated that loss of combinations of these genes results in greater impairments in neuronal migration and differentiation than does loss of any single gene alone (Deuel TAS et al., 2006; Koizumi H *et al.*, 2006). In order to test for evidence of a similar functional relationship between *Dcdc2* and *Dcx* we compared the effects of *Dcx* RNAi on $Dcdc2^{del2/del2}$ and $Dcdc2^{wt/wt}$ mutant mice. As we previously showed for *Dcx* RNAi in mice (Ramos RL et al., 2006), we found that *Dcx* RNAi delivered at E14 to wt type mice causes some cells destined for upper layers to be distributed into deeper layers in mouse neocortex, but does not lead to the formation of subcortical band heterotopia as it does in rat neocortex (Ramos RL *et al.*, 2006). Similarly, in this study, subcortical band heterotopia failed to form in any wild type mice (n=8) transfected with *Dcx* RNAi (figure 5A). In contrast to the effects of *Dcx* RNAi in $Dcdc2^{wt/wt}$ animals, 4 of 9 $Dcdc2^{del2/del2}$ mutants transfected with *Dcx* RNAi developed prominent subcortical band heterotopia in the white matter underlying neocortical lamina (figure 5B). These results indicate that the loss of *Dcdc2* function by mutations creates a sensitized

condition permissive to the formation of subcortical band heterotopia in mice upon decreased expression of *Dcx*.

To further confirm that the disruption in migration caused by *Dcx* RNAi was exacerbated in *Dcdc2* knockout mice we quantitatively compared the positions of neurons within neocortex following transfection of a scrambled control and an effective *Dcx* RNAi in $Dcdc2^{del2/del2}$ and $Dcdc2^{wt/wt}$ mice. As shown in the histogram in figure 5C, there was no significant difference between the distribution of neurons in P14 brains transfected at E15 with the scrambled control RNAi vectors in $Dcdc2^{del2/del2}$ and $Dcdc2^{wt/wt}$ mice; however, there was a significant shift in the proportion of neurons that resided in deeper positions following RNAi against *Dcx* in the *Dcdc2* knockout mice compared to wt controls (N=5, $p<0.01$). This difference was seen both in a significant decrease in cells residing in superficial layers, and a significant increase in the number of cells in deeper positions. Thus, *Dcx* RNAi impairs neuronal migration more in *Dcdc2* knockouts than in wt animals.

Dcx RNAi impairs dendritic growth and differentiation more in *Dcdc2* knockouts than in wt mice

Results from analysis of compound mutant mice for *Dcx* and *Dclk2* indicate a synergistic function for *Dclk2* and *Dcx* in the maturation of dendritic morphologies in hippocampus (Kerjan G *et al.*, 2009). We therefore assessed whether there was a similar synergistic interaction between *Dcdc2* and *Dcx* function in development of dendritic morphologies in the neocortex. For this analysis we measured the basal dendrites of layer III pyramidal neurons in somatosensory cortex in 5 brains within each of four conditions: *Dcx* shRNA in $Dcdc2^{wt/wt}$, *Dcx* shRNA scramble control in $Dcdc2^{wt/wt}$, *Dcx* RNAi in $Dcdc2^{del2/del2}$, and *Dcx* shRNA scrambled control in $Dcdc2^{del2/del2}$. We restricted the analysis to layer III neurons to avoid the possible confound of comparing displaced cells that reside in deeper layers in increased number in the $Dcdc2^{del2/del}$ *Dcx* RNAi treated mice. The results of these experiments shown in Figure 6 A-F show that *Dcx* RNAi compared to control RNAi had no effect on the mean number of primary or secondary basal dendrites in $Dcdc2^{wt/wt}$ mice (figure 6D). *Dcx* RNAi in $Dcdc2^{wt/wt}$ mice, in contrast, significantly decreased the length of basal processes both total dendritic length and length of primary, secondary and tertiary processes (figure 6 E&F; $p<0.01$). The same *Dcx* RNAi treatment in $Dcdc2^{del2/del2}$ mice, created an even greater decrease in all measures of basal dendritic process number and length ($p<0.01$). The increased severity of the *Dcx* RNAi in $Dcdc2^{del2/del2}$ mutants consisted of a complete absence of tertiary basal processes following *Dcx* RNAi (figure 6F). All measures of basal process length and number were most reduced in $Dcdc2^{del2/del2}$ mice receiving RNAi targeting *Dcx* (figure 6 D-F; $p<0.01$). Thus, similar to neuronal migration, the effects of *Dcx* RNAi on dendritic elaboration is more severe in *Dcdc2* mutants than in wild type mice.

Discussion

We report the first phenotypic description of a *Dcdc2* knockout mouse. Our assessment indicates that mutation of *Dcdc2* does not cause gross neurodevelopmental defects on its own. *Dcdc2* knockout mice breed normally, show no embryonic lethality, and display no gross disturbances in neural architecture. Consistent with normal neuroanatomic patterns in the postnatal neocortex, neurogenesis and neuronal migration in neocortex do not differ between knockouts and wild type mice. The lack of clear neurodevelopmental deficits indicate that the *Dcdc2* gene on its own is not critical to neuronal migration or neurogenesis in mice. Although there was no first order deficit in migration or neural differentiation in mouse neocortex, we did find that the effects of RNAi against *Dcx* were more severe in *Dcdc2* knockouts. This suggests that in the mouse, *Dcx* function may partially compensate for the loss of *Dcdc2*.

Members of the doublecortin family of proteins encode microtubule associated proteins that regulate cytoskeletal dynamics in developing neural cells (Koizumi H *et al.*, 2006). Genetic loss-of-function mutations in members of the DCX superfamily, *Dcx*, *Dclk*, or *Dclk2*, in mice have been found to cause far less severe developmental defects (Corbo JC *et al.*, 2002; Deuel TA *et al.*, 2006; Kerjan G *et al.*, 2009; Koizumi H *et al.*, 2006), than when mutations are combined. The compound mutants show perinatal lethality, disorganized neocortical layering, and disorganization of hippocampus (Deuel TA *et al.*, 2006; Koizumi H *et al.*, 2006). In addition, *Dcx* and *Dclk2* double knockout mice display frequent spontaneous seizures and disrupted lamination of hippocampus (Kerjan G *et al.*, 2009). These studies indicate that *Dcx* superfamily members may sometimes function in synergistic or partially redundant fashion in mice. We find a similar relationship between *Dcdc2* and *Dcx* in this study by combining RNAi of *Dcx* with *Dcdc2* mutation. The mechanism through which DCX family members cooperate is not completely clear, however, *in vitro* experiments show that all members of the family share interactions with microtubules, JIP, and neurabin, and these may serve as points of functional convergence (Reiner O *et al.*, 2006).

Interpretation of our results with *Dcdc2* knockout mice in terms of developmental learning disorders associated with *Dcdc2* should be approached with caution. The results using RNAi for three dyslexia suceptibility candidates (*Dyx1c1*, *Dcdc2*, and *Kiaa0319*) in developing rat neocortex have all suggested a connection between these candidate dyslexia susceptibility genes and neuronal migration (Burbridge TJ *et al.*, 2008; Meng H *et al.*, 2005). These findings combined with previous correlations between disruptions in neuronal migration and reading disability in humans have strengthened a hypothesis of neuronal migration disruption and dyslexia (Galaburda AM et al., 2006). It remains unknown whether function of *Dcdc2* in humans is more similar to that in rat or to that in mouse, where it is not required for migration in neocortex. As the present study is the first direct genetic test for a loss of function of *Dcdc2* mutation in any species, our results support the possibility that genetic loss of *Dcdc2* function alone need not impair neuronal migration, and that genetic variants of *Dcdc2* in humans may or may not be associated with disruptions in neuronal migration.

The *Dcdc2* knockout mouse should prove a valuable model for future studies designed to investigate the role of *Dcdc2* in neuronal physiology and behavior. As *Dcdc2* is expressed in the developing and mature brain (Burbridge TJ *et al.*, 2008; Meng H *et al.*, 2005), after neuronal migration to the neocortex has ended, *Dcdc2* may have functions in neurons beyond any role in neuronal migration. Genetic variants in *Dcdc2* in humans have now been associated significantly with dyslexia risk (Ludwig KU et al., 2008; Meng H *et al.*, 2005; Schumacher J *et al.*, 2006; Wilcke A et al., 2009), reading ability (Lind PA et al., 2010), mathematical ability (Marino C *et al.*), ADHD (Couto JM *et al.*, 2009), and speed of information processing (Luciano M et al. 2010), suggesting some as of yet undefined, and potentially pleotropic, role of *Dcdc2* in human neocortical function. Conversely, all of these cognitive functions share a functional property or properties the development of which is affected by *Dcdc2* activity. The genetic mouse model described in our present study should facilitate future studies into the role of *Dcdc2* in behavioral and neurophysiological contexts that are independent of neuronal migration.

Methods

Gene targeting and genotyping

Mice carrying the loxp-exon2-loxP conditional allele of *Dcdc2* (*Dcdc2*^{flox2}) were made by the University of Connecticut Health Center Gene Targeting and Transgenic Facility by standard methods. Briefly, embryonic stem cells harboring a floxed allele of exon two of *Dcdc2* were produced by electroporating mouse ES cells (129S6 (129SvEvTac) with a targeting construct, and subsequently drug selected and screened by PCR for correctly

targeted ES cell clones. A single positive colony was expanded and used for embryo re-aggregation to produce 5 chimeric mice. Three of these mice were shown to germline transmit the targeted allele to offspring in a cross with C57BL6 mice. The PGK-Neo cassette in the targeting construct was then removed by crossing these mice with 129S4/SvJaeSor-*Gt(ROSA)26Sor*$^{tm1(FLP1)Dym}$/J mice (JAX labs). These offspring were used to generate a colony of *Dcdc2*$^{flox2/flox2}$ mice. In order to generate *Dcdc2*$^{del2/del2}$ mice with a deletion of exon 2 we crossed *Dcdc2*$^{flox2/flox2}$ mice with Hrpt-Cre mice, C57Bl6-*Hprt*$^{tm1(cre)Mnn}$/J (UCHC). Genotyping was subsequently performed by PCR using two pairs of primers (Loxp F: 5′-agtggatctgcagggttaac, Loxp R: 5′-cttcggttgttacacgagcaat; Exon2 F: 5′-gagtggatctgcagggttaacat; Exon2 R: 5′-aagccgaggcaagcagatcttta).

RT-PCR analysis

Total RNA of the cerebral cortex was extracted from *Dcdc2*$^{del2/del2}$, *Dcdc2*$^{del2/wt}$ and *Dcdc2*$^{wt/wt}$ knock-out mice and wild-type littermates by RNAqueous (Ambion). Reverse transcription (RT) reactions were performed with 5 μg of total RNA using the SuperScript II reverse transcriptase (200 U per reaction; Invitrogen, Carlsbad, CA). RT-PCR was performed using a forward oligonucleotide primers located in *Dcdc2* exon1 (5′-atgaacggtcccagctccag) and reverse primer located in exon5 (5′-cccactccggagagttatctt') to amplify *Dcdc2* fragments spanning exon1–exon5. PCR was performed for 35 cycles with a denaturing step at 94°C (1 min), followed by annealing at 58°C (1 min) and extension at 68°C (1 min). PCR products were then purified by agarose gel electrophoresis, ligated into the PCR3.1 vector (invitrogen), and then sequenced. For quantitative real time qRT-PCR of *Dcdc2*, primers to exon 5 (tat gtg gcc gtc ggc aga g) and exon 7 (ccg atg gtt gac ttg gat tgc) were used with SYBR GREEN (Applied Biosystems) and assayed on an ABI 7500 qPCR machine (Applied Biosystems). Product amplification was validated for linearity in a serial dilution, and the expected single 98 bp amplicon was confirmed by gel electrophoresis. To quantify expression of *Dcdc2* mRNA the delta-CT from Gapdh expression (CT GAPDH-CT *Dcdc2*) was computed in triplicate technical replicates and a mean established for each of 6 brains from animals of each genotype. The primers used for GAPDH were forward (ggcaagttcaacggcacagtc) and reverse (tggtggtgaagacgccagtag).

Behavioral tests

The open field apparatus was composed of a white plastic, square-shaped (45.72 × 48.26 × 60.96 cm) enclosure. The floor was divided into a grid containing sixteen, 11.43 × 12.07 cm squares. The number of squares entered during a five minute testing period was measured by a blind observer. An entry into a field was defined as having all four paws cross the line into a square. The apparatus was cleaned with 70% EtOH after each test. A 60 × 60 cm Hebb-Williams maze (maze 1), with attached start and goal box, was constructed using black acrylic plastic; the removable floor and top were made with clear Plexiglass. One week prior to testing mice were given free access to water and restricted to 2 g of chocolate-flavored food pellets per day (Bio-Serv, Frenchtown, NJ). Mice were weighed daily and maintained at 85% of their normal body weight. During habituation, mice were allowed to explore the maze without interior walls for a maximum of 10 trials of 120 s duration. Once the subject left the start box a black plastic guillotine door was closed to prohibit re-entry. The trial ended once the mouse ate one chocolate-flavored food pellet located in the goal box, or 120s was reached. If the subject did not reach the goal box in 120s he was gently guided to the goal box, the door to the goal box was closed, and the mouse remained until one food pellet was consumed. Habituation ended when all 10 trials were completed, or the subject completed three consecutive trials in less than 30s. The next day mice were tested using the Maze 1 configuration (Meunier, 1986). The mice completed 6 trials in a maximum time of 120s per trial. ANY-maze tracking software (Stoelting) and a web camera (Logitech Quick Cam) were used to record and analyze behavior. The number of errors made during each

trial was measured. Errors were calculated when the center of mass of the subject crossed into an error zone.

Serial Section analysis and Stereological Estimate of Neuron Number in the Cerebral Cortex

After perfusion and fixation (4% paraformaldehyde) brains P40-45 were washed in water for 24 hours before being dehydrated in a series of 80%, 95%, 100% ethanol and ethanol/ether. The brains were placed into 3% celloidin for at least a week followed by 12% celloidin for 2–3 days. The celloidin block was trimmed to achieve a stable base and notched on the left side for orientation. The sections were cut coronally on a sliding microtome at 30 μm, segregated into 10 compartments, and stored in 80% ethanol. Every fifth section was stained for Nissl substance with cresyl violet. This procedure entailed washing the sections in distilled water and then placing them in 0.5% cresyl violet acetate solution (which stains the Nissl substance) for 3–5 minutes. Each section was placed in distilled water for 1 minute and then differentiated and dehydrated in 80 and 95% ethanol. A few drops of colophonium were added to the 95% ethanol baths. If differentiation was adequate, the sections were then cleared with terpineol and passed through xylol. Sections were mounted with careful attention to orientation so that left and right were identifiable consistently. The sections were then coverslipped with Permount. All cell estimations were performed under 100× oil-immersion DIC-illuminated objective using the optical fractionator as implemented by S*tereo Investigator*. Preliminary research has determined the optimal parameters for the optical fractionator. Cells are estimated using a sampling frequency of every 20^{th} section. Using a sampling grid of 530 × 530 μm, cells that lie within a counting box (15 × 15 × 20 μm) are classified as being either neurons or non-neurons (glia, blood vessel-related endothelial cells, pial, and ependymal cells). All counts were performed using standard stereologic procedures (disector/3D counting).

Histology and immunohistochemistry

For fluorescent immunostaining, brains were dissected and drop fixed for embryonic or neonatal brain, or perfusion fixed for adult with 4% paraformaldehyde/PBS. Brain sections were prepared with vibratome (Leica) at 60~80 μm and rinsed for 5 minutes in 1× PBS, blocked for 1 hr in blocking solution (1× PBS, 0.3% Triton X-100, and 5% normal goat serum), incubated either for 2 hr at room temperature or overnight at 4°C with the primary antibodies diluted in blocking solution, rinsed three times for 5 min each with 1× PBS, incubated with the appropriate secondary antibodies (Molecular probe, 1:200) diluted in blocking solution for 1 hr at room temperature, rinsed three times for 5 min each with 1× PBS, incubated 10 min with Topro3 (Molecular Probes,1;1,000), rinsed with 1× PBS, and coverslipped with Antifade (Molecular Probe, 1;3,000). Confocal images were captured using a Leica confocal microscope and imported into Adobe Photoshop. The primary antibodies were: Rabbit anti-GFP polyclonal antibody (molecular probe, 1:2,000); rabbit anti-CUX1 polyclonal anitboby, (Santa Cruz Biotechnology, 1:1,000); rabbit polyclonal anti-Tbr1 (Santa Cruz Biotechnology,1:1,000); rat polyclonal anti-Brdu (Accurate Chemical & Scientific,1;100); rabbit polyclonal anti-Ki67 (Novoacastra, 1:200); rabbit anti-phosH-3 polyclonal antibody, (Millipore, 1:200), mouse monoclonal anti-alpha tubulin (Sigma, 1: 2,000). For cilia detection the primary antibodies included a rabbit anti-ACIII (1:1000; Santa Cruz) and mouse anti-pericentrin (1:200; BD Biosciences). Quantifaction of fluorescent images was performed with ImageJ (NIH), and statistical comparisions were made by t-test for comparision of 2 groups and ANOVA for comparision of more than 2.

In Utero Electroporation

Briefly, pregnant mice were euthanized at E14, and uterus was exposed. Lateral ventricles were injected with pulled glass microcapillary needles with plasmids in a 0.01% fast green

solution (Sigma). Electrodes were placed on either side of the embryo's head, and 3× 50 ms square pulses at 25 volts were administered at 1s intervals with a BTX830 square-wave pulse generator (Genetronics, Havard Apparatus). Brains were harvested at postnatal 21 days and preceded to immunostaining and imaging analysis.

Acknowledgments

We thank the UCHC GTTF for production of the conditional *Dcdc2* allele and production of mice harboring the *Dcdc2*^{flox2} allele. This work was supported by grant HD055655 (JJL), HD057853- (AMG) and the McKnight Brain Research Foundation and the Evelyn F. and William L. McKnight Brain Institute at the University of Florida (M.R.S.).

References

Anastas SB, Mueller D, Semple-Rowland SL, Breunig JJ, Sarkisian MR. Failed cytokinesis of neural progenitors in citron kinase-deficient rats leads to multiciliated neurons. Cereb Cortex. 2011 Feb; 21(2):338–44. Epub 2010 Jun 4. [PubMed: 20525772]

Bishop GA, Berbari NF, Lewis J, Mykytyn K. Type III adenylyl cyclase localizes to primary cilia throughout the adult mouse brain. J Comp Neurol. 2007 Dec 10; 505(5):562–71. [PubMed: 17924533]

Burbridge TJ, Wang Y, Volz AJ, Peschansky VJ, Lisann L, Galaburda AM, Lo Turco JJ, Rosen GD. Postnatal analysis of the effect of embryonic knockdown and overexpression of candidate dyslexia susceptibility gene homolog *Dcdc2* in the rat. Neuroscience. 2008; 152:723–733. [PubMed: 18313856]

Corbo JC, Deuel TA, Long JM, LaPorte P, Tsai E, Wynshaw-Boris A, Walsh CA. Doublecortin is required in mice for lamination of the hippocampus but not the neocortex. J Neurosci. 2002; 22:7548–7557. [PubMed: 12196578]

Couto JM, Gomez L, Wigg K, Ickowicz A, Pathare T, Malone M, Kennedy JL, Schachar R, Barr CL. Association of attention-deficit/hyperactivity disorder with a candidate region for reading disabilities on chromosome 6p. Biol Psychiatry. 2009; 66:368–375. [PubMed: 19362708]

Deuel TAS, Liu JS, Corbo JC, Yoo SY, Rorke-Adams LB, Walsh CA. Genetic interactions between doublecortin and doublecortin-like kinase in neuronal migration and axon outgrowth. Neuron. 2006; 49:41–53. [PubMed: 16387638]

Galaburda AM, LoTurco J, Ramus F, Fitch RH, Rosen GD. From genes to behavior in developmental dyslexia. Nat Neurosci. 2006; 9:1213–1217. [PubMed: 17001339]

Kerjan G, Koizumi H, Han EB, Dube CM, Djakovic SN, Patrick GN, Baram TZ, Heinemann SF, Gleeson JG. Mice lacking doublecortin and doublecortin-like kinase 2 display altered hippocampal neuronal maturation and spontaneous seizures. Proc Natl Acad Sci U S A. 2009; 106:6766–6771. [PubMed: 19342486]

Koizumi H, Tanaka T, Gleeson JG. Doublecortin-like kinase functions with doublecortin to mediate fiber tract decussation and neuronal migration. Neuron. 2006; 49:55–66. [PubMed: 16387639]

Lind PA, Luciano M, Wright MJ, Montgomery GW, Martin NG, Bates TC. Dyslexia and *Dcdc2*: normal variation in reading and spelling is associated with *Dcdc2* polymorphisms in an Australian population sample. European journal of human genetics : EJHG. 2010

Luciano M, Hansell NK, Lahti J, Davies G, Medland SE, Raikkonen K, Tenesa A, Widen E, McGhee KA, Palotie A, Liewald D, Porteous DJ, Starr JM, Montgomery GW, Martin NG, Eriksson JG, Wright MJ, Deary IJ. Whole genome association scan for genetic polymorphisms influencing information processing speed. Biol Psychol. 86:193–202. [PubMed: 21130836]

Ludwig KU, Roeske D, Schumacher J, Schulte-Korne G, Konig IR, Warnke A, Plume E, Ziegler A, Remschmidt H, Muller-Myhsok B, Nothen MM, Hoffmann P. Investigation of interaction between *Dcdc2* and KIAA0319 in a large German dyslexia sample. J Neural Transm. 2008; 115:1587–1589. [PubMed: 18810304]

Marino C, Mascheretti S, Riva V, Cattaneo F, Rigoletto C, Rusconi M, Gruen JR, Giorda R, Lazazzera C, Molteni M. Pleiotropic effects of *Dcdc2* and DYX1C1 genes on language and mathematics traits in nuclear families of developmental dyslexia. Behav Genet. 41:67–76. [PubMed: 21046216]

Massinen S, Hokkanen Marie-Estelle, Matsson Hans, Tammimies Kristiina, Tapia-Páez I, Dahlström-Heuser V, Kuja-Panula J, Burghoorn J, Jeppsson KE, Swoboda P, Peyrard-Janvid M, Toftgård R, Castrén E, Kere J. Increased expression of the dyslexia candidate gene DCDC2 affects length and signaling of primary cilia in neurons. PLOS One.

Meng H, Powers NR, Tang L, Cope NA, Zhang PX, Fuleihan R, Gibson C, Page GP, Gruen JR. A Dyslexia-Associated Variant in *Dcdc2* Changes Gene Expression. Behavior genetics. 2010

Meng H, Smith SD, Hager K, Held M, Liu J, Olson RK, Pennington BF, DeFries JC, Gelernter J, O'Reilly-Pol T, Somlo S, Skudlarski P, Shaywitz SE, Shaywitz BA, Marchione K, Wang Y, Paramasivam M, Loturco JJ, Page GP, Gruen JR. *Dcdc2* is associated with reading disability and modulates neuronal development in the brain. Proc Natl Acad Sci USA. 2005; 102:17053–17058. [PubMed: 16278297]

Pramparo T, Youn YH, Yingling J, Hirotsune S, Wynshaw-Boris A. Novel embryonic neuronal migration and proliferation defects in *Dcx* mutant mice are exacerbated by Lis1 reduction. The Journal of Neuroscience: The Official Journal of the Society for Neuroscience. 2010; 30:3002–3012. [PubMed: 20181597]

Ramos RL, Bai J, LoTurco JJ. Heterotopia formation in rat but not mouse neocortex after RNA interference knockdown of *Dcx*. Cereb Cortex. 2006; 16:1323–1331. [PubMed: 16292002]

Reiner O, Coquelle FM, Peter B, Levy T, Kaplan A, Sapir T, Orr I, Barkai N, Eichele G, Bergmann S. The evolving doublecortin (*Dcx*) superfamily. BMC Genomics. 2006; 7:188. [PubMed: 16869982]

Schumacher J, Anthoni H, Dahdouh F, Konig IR, Hillmer AM, Kluck N, Manthey M, Plume E, Warnke A, Remschmidt H, Hulsmann J, Cichon S, Lindgren CM, Propping P, Zucchelli M, Ziegler A, Peyrard-Janvid M, Schulte-Korne G, Nothen MM, Kere J. Strong genetic evidence of *Dcdc2* as a susceptibility gene for dyslexia. Am J Hum Genet. 2006; 78:52–62. [PubMed: 16385449]

Wilcke A, Weissfuss J, Kirsten H, Wolfram G, Boltze J, Ahnert P. The role of gene *Dcdc2* in German dyslexics. Ann Dyslexia. 2009; 59:1–11. [PubMed: 19238550]

Highlights

- We produced the first knockout mouse of Dcdc2.
- We find no edivence of neuronal migration disruption in the Dcdc2 mutants.
- Dcx RNAi causes a more severe migration deficit in the Dcdc2 mutants.
- Dcx RNAi cause a more severe effect on the growth and elaboration of dendrities in the Dcdc2 mutants.
- Dcdc2 on its own is not required for neuronal migration in the neocortex, but does render the neocortex more susceptible to migration disruptions caused by Dcx RNAi.

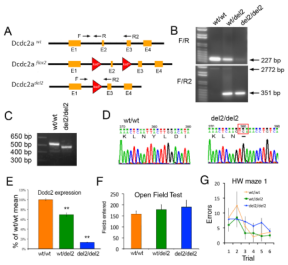

Figure 1.

The *Dcdc2* knockout and conditional knockout alleles. **A)** Schematic of wt and two mutant *Dcdc2* alleles produced for this study. The schematic also shows the position of PCR primers used for genotyping. (the genomic distances are not to scale). **B)** Example of genotyping results distinguishing between mice heterozygous or homozygous for *Dcdc2*^{wt} and *Dcdc2*^{del2} alleles. The first pair of primers (F/R) (upper panel in B) gives 227 bp PCR amplification products only in *Dcdc2*$^{wt/wt}$ and *Dcdc2*$^{wt/del2}$ animals; the second pair (F/2R) gives 2772 products in *Dcdc2*$^{wt/wt}$ and 351 bps products in dcdc$^{del2/del2}$ and *Dcdc2*$^{wt/del2}$ mice. **C)** PCR of cDNA prepared from RNA isolated from *Dcdc2*$^{wt/wt}$ or *Dcdc2*$^{del2/del2}$ mice amplified different MW products. PCR products from *Dcdc2*$^{wt/wt}$ cDNA were 547 bps and 492 bps from *Dcdc2*$^{del2/del2}$ cDNA consistent with the deletion of exon 2 in the *Dcdc2*^{del2} allele. **D)** Sequencing spectra of a region of the amplicons shown in **(C)** indicate an exon 1-3 splice variant and premature stop codon in *Dcdc2*$^{del2/del2}$ mice. **E)** Quantitative Real Time PCR results showing the expression levels of *Dcdc2* mRNA relative to expression levels in wt mice. Levels were significantly decreased in heterozygous and in homozygous mutants, consistent with potent nonsense-mediated decay. Data are expressed and percent of the mean of wt expression levels and errors are SEM. **F)** Knockout mice did not differ from wt mice in exploratory behavior. The number of fields entered was not statistically different across genotypes. Data are presented as Mean ± SEM. **G)** Deletion of *Dcdc2* does not significantly affect ability to learn a simple visuo-spatial working memory task. Plot of the mean errors (i.e. entering an error zone) across 6 learning trials in maze #1 of the Hebb-Williams maze.

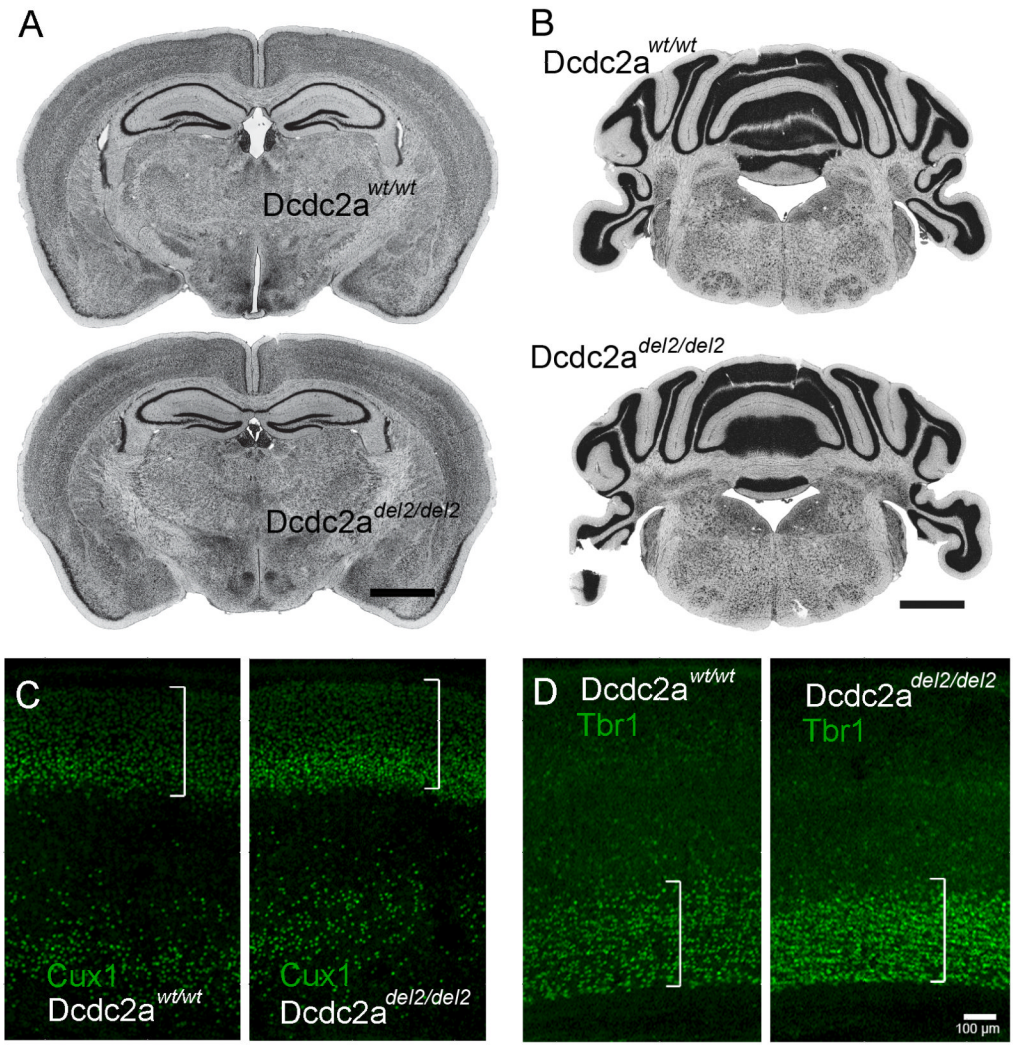

Figure 2.

Dcdc2 mutation does not result in significant developmental disruption in brain architecture or in neocortical lamination. **A)** Histology of coronal sections from adult *Dcdc2*$^{wt/wt}$ and *Dcdc2*$^{del2/del2}$ forebrain showed normal overall brain structure in *Dcdc2* knockout. Lamination of neocortex and hippocampus were preserved in the knockout. **B)** The cerebellum of *Dcdc2*$^{del2/del2}$ mice showed the pattern typical for wt cerebellum. Scale bars in A and B is 1mm. **C, D)** Immunocytochemistry for Cux1 and Tbr1 in wt and mutant neocortex at P21. Images are from somatosensory cortex at the same level and indicate no differences in the thickness of layers containing Cux1 positive cells **(C)** or TBr1 postivie cells **(D)** between *Dcdc2*$^{del2/del2}$ and *Dcdc2*$^{wt/wt}$ mice. Scale bar is 100 um and is the same for all images in C and D.

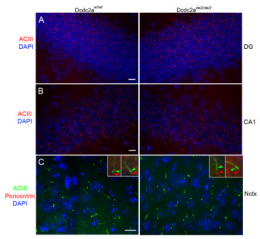

Figure 3.

Comparable neuronal primary cilia in P54 wildtype and *Dcdc2* KO cerebral cortex. (**A-C**) Confocal z-stack images of brain sections immunostained for adenylyl cyclase III (red/green) which is enriched in neuronal cilia axonemes. ACIII positive cilia were abundant in hippocampal dentate gyrus (DG) (**A**), CA1 (**B**) and neocortex (Nctx) (**C**) of both wt and KO. Insets in (**C**) show examples of neocortical cilia labeled with pericentrin (red arrowheads) and ACIII (green arrowheads) in both wt and KO. Pericentrin is a basal body marker that asymmetrically localizes to the base of ACIII+ axonemes. All nuclei were labeled with DAPI. Scale bars =10μm.

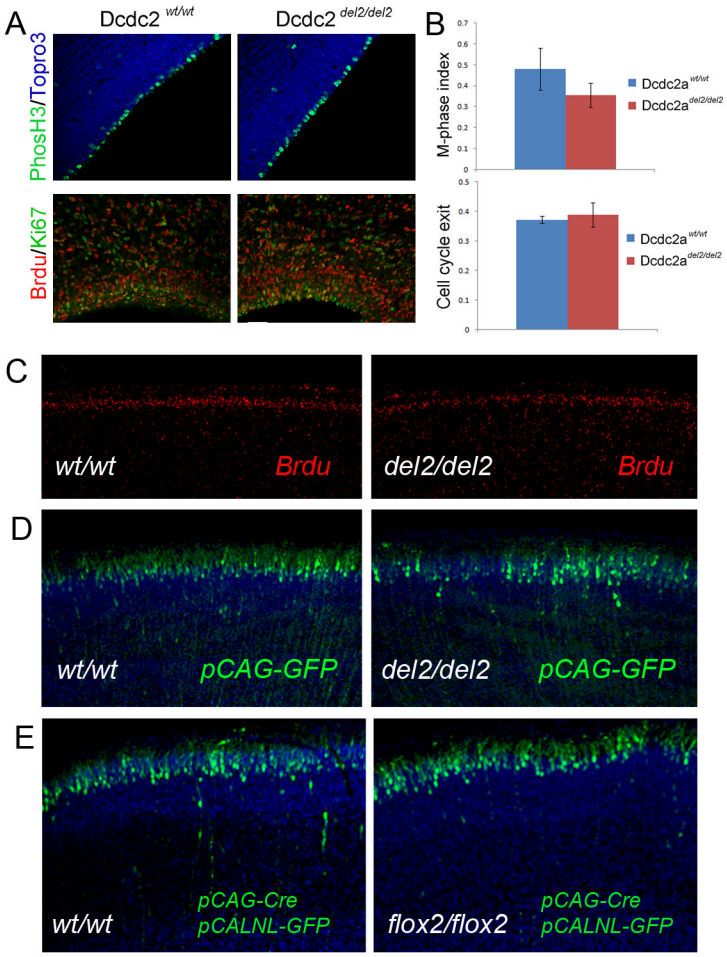

Figure 4.

No significant differences in neurogenesis or neuronal migration in fetal neocortex in *Dcdc2* knockouts. **A)** M-phase cells labeled with phos-H3 in E15 neocortex are shown in the upper panel for both wt and KO. Nuclei are labeled by Topro3. The lower panel in **(A)** shows BrdU and Ki67 immuno-labeling 24 hours after a BrdU injection at E14. **B)** Bar graphs of the quantification of experiments depicted in **(A)** for mitotic cells (upper graph, and the fraction of cells that exited the cell cycle in 24 hours (bottom graph). There were no significant difference in either the fraction of cells at the VZ surface that are positive for Phos-H3 (M-phase-index) (N=5, $p>0.05$), nor was there a significant difference in the fraction of BrdU labeled cells that were negative for Ki67 (cells that exited the cell cycle) (N=5 $p>0.05$). **C)** The position of neurons in neocortex labelled with BrdU at E15 and examined 6 days later show similar migration to upper layers of neocortex in *Dcdc2*$^{wt/wt}$ and *Dcdc2*$^{del/del}$ mice. **D)** Position of eGFP labeled neurons 6 days following electroporation at E15 in *Dcdc2*$^{wt/wt}$ and *Dcdc2*$^{del/del}$ mice. All labeled neurons were in similar upper layer positions in both wt and knockout animals. **E)** Conditional genetic deletion in migrating neocortical pyramidal neurons in *Dcdc2*$^{flox2/flox2}$ did not result in impaired migration. A Cre-recombinase expressing plasmid (pCAG-Cre) and a reporter plasmid that expresses GFP after Cre recombination (pCALNL-GFP) was transfected into wt and animals homozygous for the floxed allele *Dcdc2*^{flox2}. The position of neurons examined 6 days later on the day of birth have the same migration pattern into upper layers.

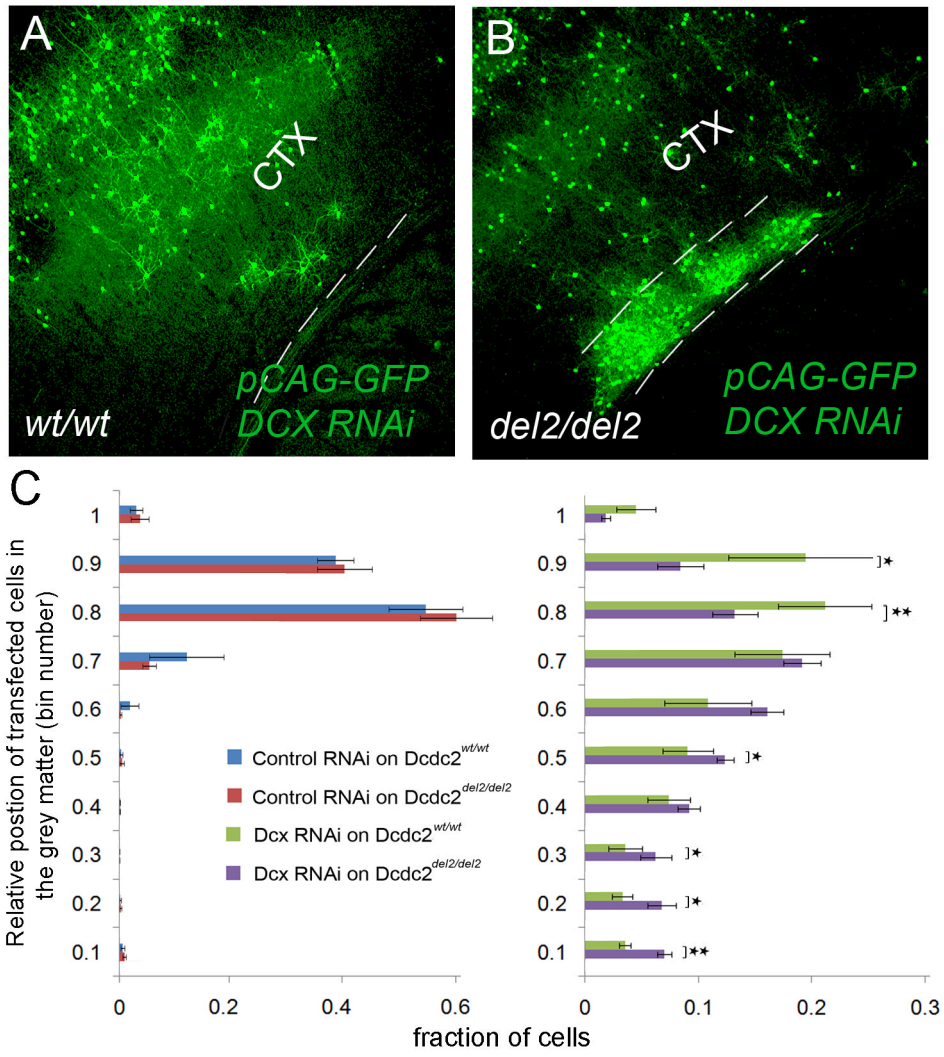

Figure 5.

Enhanced migration disruptions by *Dcx* RNAi in *Dcdc2* KO mice. **A-B)** P14 cortex in the region of somatosensory neocortex following transfection of a *Dcx* shRNA plasmid and a GFP expression plasmid at E14 in a wt **(A)** and *Dcdc2* knockout littermate **(B)**. In both transfections cells are not within the expected upper layer positions, and in the *Dcdc2*$^{del2/del2}$ mutant there is an aggregation of neurons in the white matter that form a subcortical heterotopia (between dotted line in B). **C)** Histograms showing normalized distributions of neurons in neocortical at P14 following transfection of *Dcx* shRNA and a control shRNA in wt and *Dcdc2* knockout animals (N=5 for each condition). Histograms show the percent of transfected (eGFP+) neurons contained within each of the position deciles the layer VI white matter boundary (0.1) to the pial surface (1) (neurons in subcortical heterotopia present in knockout were not included in this analysis because they fall below the whitematter layer 6 boundary). Statistical analysis of the distribution revealed a significant difference in the pattern of neuronal positions in *Dcx* RNAi (green and purple bars) and control RNAi (red and blue bars) in both genotypes (ANOVA, position as a repeated measure, $p<0.001$), and a significant difference in the distribution between the position of *Dcx* RNAi treated cells in *Dcdc2*$^{wt/wt}$ (green bar) and *Dcdc2*$^{del/del}$ (purple bars) (ANOVA, position as a repeated measure, $p<0.01$). In particular, in *Dcx* RNAi in *Dcdc2* knockouts there were significantly

greater fractions of neurons in the lower deciles with a smaller fraction in the upper decile, compared wot *Dcx* RNAi treated cells in the wild type cortex.

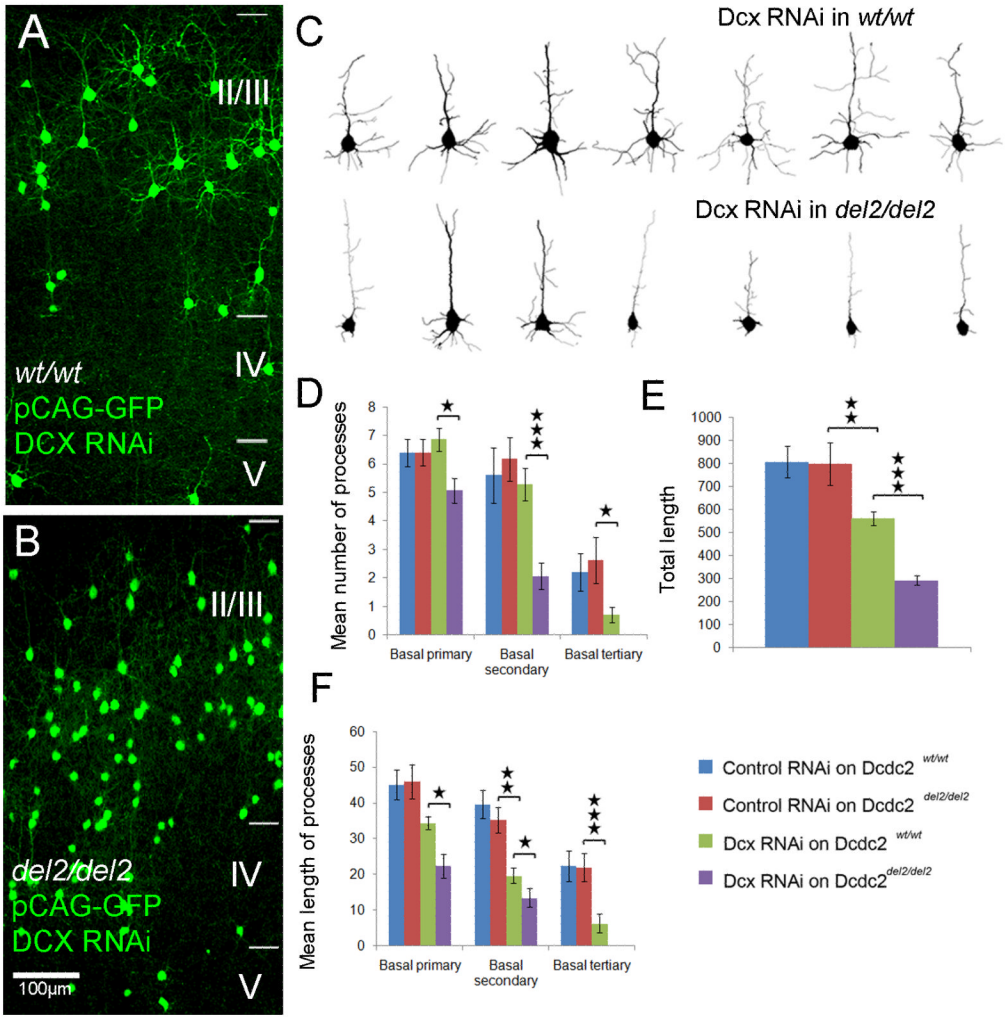

Figure 6.

Dcx RNAi reduces dendritic growth and elaboration in layer 3 pyramidal neurons in *Dcdc2* knockouts more than in wildtypes. Images of GFP transfected neurons in neocortex from **(A)** *Dcdc2*a$^{wt/wt}$ and **(B)** *Dcdc2*a$^{del2/del2}$ animals that were electroporated with *Dcx* RNAi at E15 and examined at P25. Images are from somatosensory cortex. **(C)** Example of reconstructed layer 3 cortical neurons transfected with *Dcx* RNAi in *Dcdc2*a$^{wt/wt}$ (upper row) or *Dcdc2*a$^{del2/del2}$ (lower row) mice. The reconstructions of proximal dendritic arborizations was use to analyze the lenth and number of denddritic processes following *Dcx* RNAi is *Dcdc2* knockouts and wild type animals. **(D-F)** Bar graphs of number **(D)** total number, **(E)** total length and **(F)** mean length of secondary and tertiary basal dendrites in the four indicated conditions. The morphology of neurons in wt or knockout did not differ in any measures with control, scrambled RNAi transfections (red and blue bars), and *Dcx* RNAi transfection in *Dcdc2* knockout mice had the greatest reduction in dendritic arborization (purple bars).